

## Spatio-Temporal Signal Subspace-Based Subband Space-time Adaptive Antennas

Kehu Yang <sup>1</sup>, Yimin Zhang <sup>2</sup>, and Yoshihiko Mizuguchi <sup>1</sup>

<sup>1</sup> ATR Adaptive Communications Research Laboratories  
Seika-cho, Souraku-gun, Kyoto 619-0288, Japan  
E-mail: {yang,mizu}@acr.atr.co.jp

<sup>2</sup> Department of Electrical and Computer Engineering  
Villanova University, Villanova, PA 19085, USA  
E-mail: yimin@ieee.org

### 1. Introduction

Inter-symbol interference (ISI) and cochannel interference (CCI) are two main problems which limit the communication quality and capacity in mobile communication systems. The adaptive antenna under space-time adaptive processing (STAP) is considered as an efficient way in solving those problems. However, due to the large scale of adaptive weights and the high correlation in space and time, such an adaptive antenna suffers from the large computation burden and the slow convergence performance.

To ease these problems of STAP, the authors have proposed the subband adaptive array scheme [1, 2], which, in essence, is an equivalent space-frequency domain approach to STAP. In this paper, we propose a novel approach of the spatio-temporal signal subspace-based subband space-time adaptive processing (SSTAP) scheme. Compared with the conventional STAP, the proposed method greatly improves the convergence performance, while the performance of the residual error power remains unchanged.

### 2. Signal Model

Consider a base station using an antenna array of  $N$  ( $N \geq 1$ ) elements. Signals from  $P$  ( $P \geq 1$ ) users are illuminating the array. The signal of the desired user is denoted as  $s_1(t)$ , whereas the signals from other users are denoted as  $s_p(t)$ ,  $p = 2, \dots, P$ . The received signal vector at the array is expressed as

$$\mathbf{x}(t) = \sum_{p=1}^P \sum_{m=-\infty}^{+\infty} s_p(m) \mathbf{h}_p(t - mT) + \mathbf{n}(t) \quad (1)$$

where  $s_p(m)$  and  $\mathbf{h}_p(t)$  are the information symbol sequence and the channel vector of the  $p$ -th user,  $T$  denotes the symbol duration, and  $\mathbf{n}(t)$  is the array noise vector. In the following, we use  $(\cdot)^*$ ,  $(\cdot)^T$  and  $(\cdot)^H$  to express complex conjugate, transpose and conjugate transpose, respectively.

To simplify the subsequent analysis, we make the following assumptions.

A1) The user signals are wide-sense cyclostationary when they are sampled at fractionally spaced symbol cycle, and are wide-sense stationary when they are sampled at the symbol rate.

A2) The information symbols  $s_p(m)$ ,  $p = 1, \dots, P$  are i.i.d. (independent and identically distributed)

with  $E\{|s_p(m)|^2\} = 1$ , and are uncorrelated with the channel noise vector.

A3) All channels  $\{\mathbf{h}_p(t), p = 1, \dots, P\}$  are linear and time-invariant, and each of them is of a finite duration within  $[0, D_p T]$ , where  $D_p$  is called the channel order of the  $p$ -th user.

A4) The noise vector is zero-mean, temporally and spatially white with circular Gaussian property.

Denote  $\Delta$  as the sampling cycle, and let  $J = T/\Delta$  ( $J \geq 1$ ). Further, we denote  $\underline{\mathbf{x}}(n) = [\mathbf{x}^T(nT), \mathbf{x}^T(nT - \Delta), \dots, \mathbf{x}^T(nT - (J-1)\Delta)]^T$ , then

$$\underline{\mathbf{x}}(n) = \sum_{p=1}^P \sum_{d=0}^{D_p} s_p(n-d) \underline{\mathbf{h}}_p(d) + \underline{\mathbf{n}}(n) \quad (2)$$

where  $\underline{\mathbf{h}}(n) = [\mathbf{h}^T(nT), \dots, \mathbf{h}^T(nT - (J-1)\Delta)]^T$  and  $\underline{\mathbf{n}}(n) = [\mathbf{n}^T(nT), \dots, \mathbf{n}^T(nT - (J-1)\Delta)]^T$ . For  $M$  consecutive symbol periods, we denote

$$X(n) = [\underline{\mathbf{x}}^T(n), \dots, \underline{\mathbf{x}}^T(n-M+1)]^T = \sum_{p=1}^P \mathbf{H}_p S_p(n) + N(n) \quad (3)$$

as the input vector of the entire STAP system, where  $S_p(n) = [s_p(n), s_p(n-1), \dots, s_p(n-M-D_p+1)]^T$ ,  $N(n) = [\underline{\mathbf{n}}^T(n), \underline{\mathbf{n}}^T(n-1), \dots, \underline{\mathbf{n}}^T(n-M+1)]^T$ , and

$$\mathbf{H}_p = \begin{bmatrix} \underline{\mathbf{h}}_p(0) & \dots & \underline{\mathbf{h}}_p(D_p) & \mathbf{0} & \dots & \dots & \mathbf{0} \\ \mathbf{0} & \underline{\mathbf{h}}_p(0) & \dots & \underline{\mathbf{h}}_p(D_p) & \mathbf{0} & \dots & \mathbf{0} \\ \vdots & \ddots & \dots & \ddots & \dots & \ddots & \vdots \\ \mathbf{0} & \dots & \dots & \mathbf{0} & \underline{\mathbf{h}}_p(0) & \dots & \underline{\mathbf{h}}_p(D_p) \end{bmatrix}$$

Let  $W$  be the weight vector to  $X(n)$ , the output of space-time adaptive processing is given by

$$y(n) = W^T X(n) \quad (4)$$

Under the minimum mean square error (MMSE) criterion, the optimum weights of the STAP are given by the well-known Wiener-Hopf solution

$$W_{MMSE}^* = \mathbf{R}_X^{-1} \mathbf{r}(v) \quad (5)$$

where  $\mathbf{R}_X = E[X(n)X^H(n)]$ ,  $\mathbf{r}(v) = E[s_1^*(n-v)X(n)]$ , and  $v \geq 0$  is a proper delay of the training signal, which is assumed to be an ideal replica of the desired signal  $s_1(n)$ .

### 3. Subspace Decomposition

Under the assumptions A1) – A4), the correlation matrix of the signal vector can be rewritten as

$$\mathbf{R}_X = E[X(n)X^H(n)] = \mathbf{H}\mathbf{R}_S\mathbf{H}^H + \mathbf{R}_N \quad (6)$$

where  $\mathbf{H} = [\mathbf{H}_1 \mathbf{H}_2 \dots \mathbf{H}_P]$ ,  $\mathbf{R}_S = \text{Diag}\{\mathbf{R}_p, p=1, \dots, P\} = \mathbf{I}_{M_D}$ ,  $\mathbf{R}_p = E[S_p(n)S_p^H(n)] = \mathbf{I}_{M+D_p}$ ,  $\mathbf{R}_N = E[N(n)N^H(n)] = \sigma^2 \mathbf{I}_{MNJ}$ ,  $M_D = \sum_{p=1}^P (M + D_p)$ , and  $\mathbf{I}_M$  is the  $M \times M$  identity matrix. Performing eigen-decomposition to  $\mathbf{R}_X$  yields

$$\mathbf{R}_X = \mathbf{S}\Sigma_s\mathbf{S}^H + \mathbf{G}\Sigma_n\mathbf{G}^H \quad (7)$$

where  $\lambda_1 \geq \lambda_2 \geq \dots \geq \lambda_{M_D} \geq \lambda_{M_D+1} = \dots = \lambda_{MNJ} = \sigma_n^2$  are the eigenvalues of  $\mathbf{R}_X$ , and  $\Sigma_s = \text{diag}\{\lambda_i, i=1, \dots, M_D\}$ ,  $\Sigma_n = \text{diag}\{\lambda_i, i=1+M_D, \dots, MNJ\}$ . The columns of  $\mathbf{S} = [\mathbf{S}_1, \dots, \mathbf{S}_{M_D}]$  span the spatio-temporal signal subspace, whereas the columns of  $\mathbf{G} = [\mathbf{G}_1, \dots, \mathbf{G}_{MNJ-M_D}]$  span the spatio-temporal noise subspace.

### 4. Spatio-temporal Signal Subspace-based Subband Processing Schemes

According to A2, it is seen that  $\mathbf{r}(v)$  is the  $(v+1)$ -th column of  $\mathbf{H}_1$ , which means  $\mathbf{r}(v)$  belongs to the signal subspace spanned by the columns of  $\mathbf{S}$  or  $\mathbf{H}$ . Using the orthogonality property between the signal subspace and its noise subspace, the residual error power of (4) under (5) can be denoted as

$$\sigma_{MMSE}^2 = E|s_1(n-v) - y(n)|^2 = 1 - W_{MMSE}^T \mathbf{R}_X W_{MMSE}^* = 1 - \mathbf{r}^H(v) \mathbf{S} \Sigma_s^{-1} \mathbf{S}^H \mathbf{r}(v) \quad (8)$$

which tells the fact that for STAP, using the projection of the received signal vector on the spatio-temporal signal subspace instead of the received signal vector itself does not reduce the output performance of the residual error power. For fair comparison, under the polyphase representation [4,5] we define the relation between the conventional STAP filter and the signal subspace-based STAP filter by

$$\begin{bmatrix} \mathbf{W}_1(z^L) \\ \vdots \\ \mathbf{W}_M(z^L) \end{bmatrix} = \mathbf{S}^* \times \begin{bmatrix} \mathbf{F}_1(z^L) \\ \vdots \\ \mathbf{F}_K(z^L) \end{bmatrix} \quad (9)$$

where  $\mathbf{W}_l(z) = \sum_{n=0}^{K-1} z^{-n} \underline{\mathbf{w}}_{nL+l-1}$ , and  $\mathbf{W}(z) = \sum_{l=0}^{M-1} z^{-l} \underline{\mathbf{w}}_l = \sum_{l=1}^M z^{-(l-1)} \mathbf{W}_l(z^L)$ , and  $M = (K-1)L + \underline{M}$  and

$1 \leq L \leq \underline{M}$ . It will be seen that (9) yields the signal subspace-based subband approach.

To obtain the subband realization, we partition  $\mathbf{S}$  into  $M \times M_t$  submatrices as following,

$$\mathbf{S} = [\mathbf{S}_1, \mathbf{S}_2, \dots, \mathbf{S}_{M_t}] = \begin{bmatrix} \mathbf{S}_{11} & \cdots & \mathbf{S}_{1M_t} \\ \vdots & \ddots & \vdots \\ \mathbf{S}_{M1} & \cdots & \mathbf{S}_{MM_t} \end{bmatrix} \quad (10)$$

where  $\mathbf{S}_{ij}$ ,  $i = 1, \dots, M$ ,  $j = 1, \dots, M_t$ , are the submatrices of  $\mathbf{S}$ , each submatrix dimension is  $NJ \times NJ$  and  $M_t (= M_D/NJ)$  is the dimension of the signal subspace. In practice, the dimension can be estimated by using the information criteria such as the Akaike Information Criterion (AIC).

By using the polyphase representation [4, 5], the  $z$ -transform of the output of the signal subspace-based system can be expressed as

$$Y(z) = \sum_{j=1}^{M_t} \sum_{i=1}^M z^{-(i-1)} \mathbf{F}_j^T(z^L) \mathbf{S}_{ij}^H \underline{\mathbf{x}}(z) = \sum_{j=1}^{M_t} \mathbf{F}_j^T(z^L) \mathbf{G}_j^T(z) \underline{\mathbf{x}}(z) \quad (11)$$

where  $Y(z)$  is the  $z$ -transform of  $y(n)$ ,  $\underline{\mathbf{x}}(z)$  express the  $z$ -transform of  $\underline{\mathbf{x}}(n)$ , and

$$\mathbf{G}_j(z) \triangleq \sum_{i=1}^M z^{-(i-1)} \mathbf{S}_{ij}^*, \quad \mathbf{F}_j(z) \triangleq \sum_{l=1}^2 \mathbf{f}_{jl} z^{-(l-1)} \quad (12)$$

in which two-tap filters are used for the new subband filters  $\mathbf{F}_j(z)$ . We call  $\mathbf{G}_j(z)$  as the space-time subband filter. Under the subband STAP, it is seen from the aforementioned definition of  $\mathbf{W}(z)$  under the line of (9) that the equivalent number to the delay line taps of the conventional STAP filter is  $(2-1) \times L + M_t$ . Using vector notations, (11) can be expressed in the time domain as

$$y(n) = \sum_{l=0}^1 \mathbf{f}_l^T \bar{\mathbf{x}}(n - lL) \quad (13)$$

where  $\mathbf{f}_l = [\mathbf{f}_{1l}^T, \dots, \mathbf{f}_{M_t l}^T]^T$  and  $\bar{\mathbf{x}} = [\bar{\mathbf{x}}_1^T, \dots, \bar{\mathbf{x}}_{M_t}^T]^T$ , and  $\bar{\mathbf{x}}_j(n)$  is the output of subband filter  $\mathbf{G}_j(z)$ .

## 5. Convergence Rate Analysis

Using the LMS algorithm, the weights of STAP in (5) is updated according to

$$W^{(k+1)} = W^{(k)} + \mu e^*(n) X(n) \quad (14)$$

where  $\mu$  is the step size, and  $e(n) = s_1(n-v) - y(n)$  is the error signal. For the proposed subband STAP, due to the decorrelation by the subband filtering, each weight can be updated under the LMS algorithm with the different step size,

$$\mathbf{f}_l^{(k+1)} = \mathbf{f}_l^{(k)} + \mu \Sigma_s^{-1} \Phi e^*(n) \bar{\mathbf{x}}(n - lL), \quad l = 0, 1. \quad (15)$$

In the case of uncorrelated signals, the diagonal elements of  $\Sigma_s$  represent the power of the uncorrelated subband channel signals. Let  $\mathbf{f}_\alpha = [\mathbf{f}_0^T, \mathbf{f}_1^T]^T$  and  $\mathbf{x}_\alpha(n) = [\bar{\mathbf{x}}^T(n), \bar{\mathbf{x}}^T(n-L)]^T$ , (15) can be written as

$$\mathbf{f}_\alpha^{(k+1)} = \mathbf{f}_\alpha^{(k)} + \mu \Lambda e^*(n) \mathbf{x}_\alpha(n) \quad (16)$$

where  $\Lambda = \mathbf{I}_2 \otimes \Sigma_s^{-1}$ , and  $\otimes$  expresses the Kronecker product. From the general convergence analysis of the LMS algorithm, the convergence rate of the LMS algorithm based on (16) mainly depends on the eigenvalue spread of the weighted correlation matrix  $\mathbf{R}_\alpha = E[\Lambda \mathbf{x}_\alpha(n) \mathbf{x}_\alpha^H(n)]$ . To compare  $\mathbf{R}_\alpha$  with  $\mathbf{R}_x$ , it is seen that the eigenvalue spread of  $\mathbf{R}_\alpha$  is much smaller than that of  $\mathbf{R}_x$ . So the convergence rate of (16) is highly improved. It is noted that the existence of  $\min\{M_D - L, NJM_t - NJL\}$  zero eigenvalues of  $\mathbf{R}_\alpha$  does not influence the convergence rate of the LMS algorithm [5]. The presence of zero eigenvalues brings an infinite number of optimum solutions in terms of the Wiener-Hopf solution (5) with the same residual power.

## 6. Simulation Results

In the simulation, a uniform circular array with three identical point elements is employed. The inter-element spacing is  $\sqrt{3}\lambda$  ( $\lambda$  is the RF wavelength). Three users are present, where one is the desired user

and the others are interference users. All of the user signals are modulated by QPSK with an FIR of roll-off factor 1.0. Each user has six rays arriving at the array with different elevation  $\theta$  and azimuth  $\varphi$ . The parameters for those three users are listed in Table I, where  $\tau$  and  $\xi$  denote the time delay and propagation loss, respectively. The input SNR of the first ray of each user is 10 dB.

The LMS algorithm is employed and the step size for both STAP and SSTAP algorithms is selected as  $\mu=0.4/(\text{total input power})$ . The total power for the STAP and SSTAP equals to the trace of  $\mathbf{R}_X$  and the trace of  $\mathbf{R}_\alpha$ , respectively. We assume  $J=2$  and  $M=20$ . Further, in each subband, two taps ( $K=2$ ) are taken, and  $L$  is selected to meet  $M = (2 - 1) \times L + M_l$ .

Fig. 1 shows the residual error power versus the number of iteration. To evaluate the effect of the estimated spatio-temporal signal subspace on the output performance of SSTAP,  $N_t = 220, 520,$  and  $1020$  samples are used for the signal subspace estimation, and the performance is shown as  $\text{SSTAP}_1, \text{SSTAP}_2,$  and  $\text{SSTAP}_3,$  respectively. From this figure, two observations are in order. (1) All the three types of SSTAP provide high convergence rate than that of the conventional STAP. (2) The larger number of samples is used for the estimation of the signal subspace, the higher the convergence rate.

To show the reduction of the eigenspread by SSTAP, we plotted in Fig. 2 the eigenvalues of the associated correlation matrix. This figure clearly shows the significant reduction of the eigenvalue spread by using the spatio-temporal signal subspace-based subband approach.

## 7. Conclusion

We have proposed the spatio-temporal signal subspace-based subband approach to the conventional STAP. Theoretical analysis and computer simulations have shown that the proposed approach greatly improves the convergence rate whereas the steady-state performance remains unchanged.

## References

- [1] Y. Zhang, K. Yang, and M. G. Amin, "Performance analysis of subband adaptive arrays in multipath propagation environment," in *Proc. IEEE Signal Processing Workshop on Statistical Signal and Array Processing*, Portland, OR, pp. 17-20, Sept. 1998.
- [2] Y. Zhang, K. Yang, and Y. Karasawa, "Subband CMA adaptive arrays in multipath fading environment," *IEICE Trans. Commun.*, vol. J82-B, no. 1, pp. 97-108, Jan. 1999.
- [3] Haykin, *Adaptive Filter Theory*, 3rd Ed. Prentice Hall, 1996.
- [4] P. P. Vaidyanathan, *Multirate Systems and Filter Banks*, Prentice Hall, 1993.
- [5] M. R. Petraglia and S. K. Mitra, "Adaptive FIR filter structure based on the generalized subband decomposition of FIR filters," *IEEE Trans. Circuits & Systems-II: Analog and Digital Signal Processing*, vol. 40, pp. 354-362, June 1993.

No.	$\theta$ (deg.)	$\varphi$ (deg.)	$\tau$ (sym.)	$\xi$
1	-12.3	24.6	0	1.0
2	-28.0	30.7	0.99	0.02-0.84i
3	-13.1	46.7	1.16	0.09+0.80i
4	-0.80	13.0	3.89	-0.75-0.26i
5	-24.0	48.8	5.69	-0.54-0.44i
6	-26.0	25.9	7.41	-0.52-0.29i

Table I (a) desired signal

No.	$\theta$ (deg.)	$\varphi$ (deg.)	$\tau$ (sym.)	$\xi$
1	-8.6	33.6	0	1.0
2	-21.7	46.8	0.65	0.78+0.06i
3	-21.2	77.1	1.09	0.65-0.33i
4	-27.2	67.0	6.43	-0.58-0.17i
5	-10.9	76.8	6.69	0.06+0.54i
6	-26.0	59.0	9.46	-0.39-0.34i

Table I(b) Interference signal 1

No.	$\theta$ (deg.)	$\varphi$ (deg.)	$\tau$ (sym.)	$\xi$
1	-6.6	120.6	0	1.0
2	-3.3	147.3	1.29	0.04+0.86i
3	-8.7	125.2	1.74	0.26+0.79i
4	-9.4	151.9	5.73	0.70+0.29i
5	-14.0	124.8	6.47	0.49+0.06i
6	-0.30	159.3	8.15	-0.37-0.25i

Table I(c) Interference signal 2

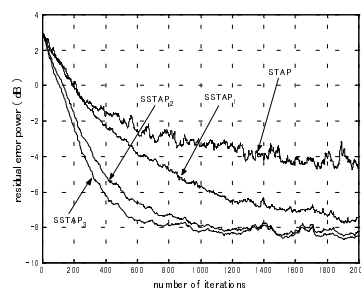
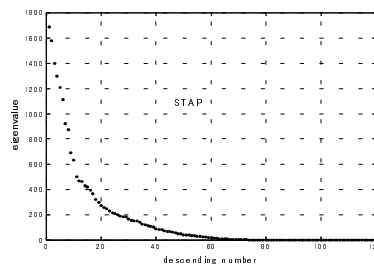
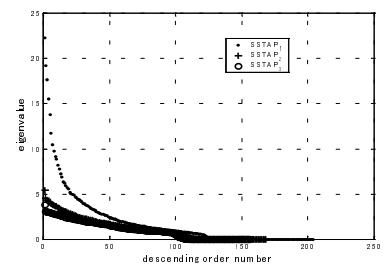


Fig. 1 Convergence curves



(a) STAP



(b) SSTAP

Fig. 2 Eigenvalue spectra